NETWORKS AND HETEROGENEOUS MEDIA
©American Institute of Mathematical Sciences
Volume **2**, Number **4**, December **2007**

Website: http://aimSciences.org

pp. **733–750**

ADJOINT CALCULUS FOR OPTIMIZATION OF GAS NETWORKS

Michael Herty

Technische Universität Kaiserslautern
Fachbereich Mathematik
Postfach 3049
D-67653 Kaiserslautern, Germany

Veronika Sachers

Technische Universität Kaiserslautern
Fachbereich Mathematik
Postfach 3049
D-67653 Kaiserslautern, Germany

Abstract. We consider an optimization problem arising in the context of gas transport in pipe networks. To compensate the pressure loss due to friction and to guarantee a desired (time dependent) outflow profile, compressor stations are included in the network. These compressor stations are relatively cost-intensive, so that a cost effective control is required. In the presented model the compressors are special vertices of the network. We derive an adjoint calculus for gas networks to solve the optimization problem and prove well–posedness of forward and adjoint coupling conditions. Furthermore, numerical examples illustrate the obtained results.

1. **Introduction.** Recently, there has been intense research in physical phenomena posed on networks with applications in gas dynamics [5, 6, 12, 13, 14, 16, 30, 35] and other areas as for example traffic flow [8, 11, 19, 28, 29] or networks of open channels [23, 24]. Recent work has also been conducted in the field of telecommunication networks [2] and supply chains [1, 3, 4, 20].

This publication is concerned with the optimal control of gas networks which is an important industrial problem and has been under investigation for several years, see [17, 25, 37, 38, 40, 41]. Further control problems in the context with networks have been studied in the case of traffic flow e.g. in [18, 26, 27] and in [22] for water networks. In gas networks the basic physical phenomenon is pressure loss due to pipe wall friction effects. Therefore, compressor stations are introduced at certain points in the network raising again the pressure. One question arising in this context is the optimal (i.e. cost effective) choice of the pressure energy which has to be applied to satisfy certain pressure demands of customers. In this context models for transient gas flow have been investigated recently, see e.g. [17, 35]. Therein, discretized flow equations are used and solved by linear [21, 43, 45], mixed–integer [35] or nonlinear optimization techniques [17]. We contribute to this discussion by

2000 *Mathematics Subject Classification.* Primary: 76N25; Secondary: 35Lxx.
Key words and phrases. Isothermal Euler equations, Networks, Flow control.
This work has been supported by grant DFG SPP 1253 and by grant DAAD D/06/28176.

considering a simplified model in a *continuous* setting. Well–posedness of the model equations is shown. We investigate the approach of optimize–then–discretize in the following sense: We first derive an adjoint calculus for a particular gas network model. Then, we prove well–posedness of the arising coupling conditions in the continuous optimality system. This guarantees that the optimality system can be discretized. We finally discretize and solve numerically the optimality system on a sample network and compare the results with another coarse scale model for optimization of gas pipelines.

The outline of the paper is as follows. Section 2 deals with the modeling part. We motivate the use of a simplified model for gas transport in networks and introduce the basic notations for the network model. Further, a detailed analysis of the equations is given. Section 3 is devoted to the optimization of this model and Section 4 contains the numerical results. We summarize the results in Section 5.

2. **Common Gas Models For Pipe Networks.**

We introduce the governing dynamics for gas flow in pipe networks and some necessary notation.

In case of a single pipe and natural gas flow some common assumptions include constant temperature of the gas. Further the pipe is modeled as an only one–dimensional domain, see [37, 38, 40]. This allows to simplify the Euler equations and obtain the following set of partial differential equations

$$\partial_t \rho + \partial_x(\rho u) = 0, \tag{1a}$$

$$\partial_t(\rho u) + \partial_x(\rho u^2 + p(\rho)) = -f_g \frac{\rho u|\rho u|}{2D\rho}, \tag{1b}$$

where $\rho(x,t)$ is the gas density u the gas velocity and $p(\rho)$ an equation of state. In the momentum equation we have a steady state friction factor f_g calculated for example using Chen's formula [10]. The diameter of the pipe is D. Moreover, in many cases the term $\partial_x\left(\rho u^2\right)$ in (1) can be neglected, see [37]. This simplification can be justified when considering realistic high–pressure gas systems: Typical values are $u \approx 10[m/s]$, $c \approx 300[m/s], \rho = 50[kg/m^3]$ and $p = 70$ $[bar]$. For a pipe of length $L = 100[km]$ and a time period of $t = 1[h]$, the momentum term $\partial_x \rho u^2$ is of order $O(10^{-3})$, whereas all other terms (and in particular the friction term) is of order $O(1)$. The pipe wall friction factor f_g is typically of order $O(10^{-2})$. This derivation is only formal and not mathematically justified. However, the simplified equations are commonly used in the engineering community [39, 44]. In the section on numerical results we give a comparison of model (1) and its simplified version (2).

From now on, we consider this simplified model for gas transport.

$$\partial_t \rho + \partial_x(\rho u) = 0 \tag{2a}$$

$$\partial_t(\rho u) + \partial_x p(\rho) = -f_g \frac{\rho u|\rho u|}{2D\rho}. \tag{2b}$$

The equation of state typically applied in the context of gas flow at constant temperature is given by

$$p(\rho) = \frac{z\mathcal{R}T}{M_g}\rho =: a^2\rho, \tag{3}$$

where p is the pressure, z the natural gas compressibility factor, $\mathcal{R}$ the universal gas constant, M_g the molecular weight of the gas and $\mathcal{T}$ the temperature of the gas. The resulting parameter a can be viewed as the speed of sound in the gas. It describes the speed of propagation of simple waves in solutions to model (2).

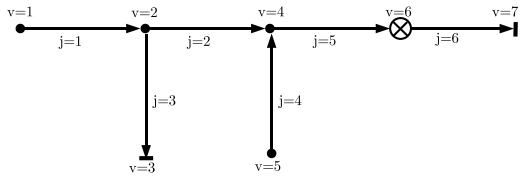

FIGURE 1. Illustration of the directed graph as model for a pipe network

Throughout the document we use the following notation

$$q := \rho u,\ U := \begin{pmatrix} \rho \\ q \end{pmatrix},\ F(U) := \begin{pmatrix} q \\ a^2\rho \end{pmatrix}. \tag{4}$$

We recall basic properties of (2) and equation (3). The eigenvalues are $\lambda_{1/2} = \pm a$ and the corresponding eigenvectors are given by $r_{1/2} = \begin{pmatrix} 1 \\ \pm a \end{pmatrix}$. A parameterization of the i-contact discontinuity curves through a given state U_l is hence given by

$$U_i(\xi) = U_l + \xi r_i = U_l + \xi \begin{pmatrix} 1 \\ \pm a \end{pmatrix} \quad -\infty < \xi < \infty. \tag{5}$$

The single model can be extended to a network as follows: We call a finite, directed graph $(\mathcal{J}, \mathcal{V})$ a network. Both sets are supposed to be non–empty sets of indices. Each element (edge) $j \in \mathcal{J}$ corresponds to a pipe. Each pipe is parameterized by a finite interval $\mathcal{I}_j := [x_j^a, x_j^b]$. Each element (node) $v \in \mathcal{V}$ correspond to a single intersection of pipes. We refer to figure 1 for an example. For a fixed vertex $v \in \mathcal{V}$, $\delta_v^-(\delta_v^+)$ is defined as the set of all indices of edges $j \in \mathcal{J}$ ingoing (outgoing) to the vertex v. We given an example: For the vertex $v = 2$ of figure 1 we have $\delta_2^- = \{1\}, \delta_2^+ = \{2, 3\}$. Note that for the vertex $v = 1$ and $v = 5$, the set $\delta_v^- = \emptyset$ since these vertices are inlets. A similar argument holds true for the vertices $v = 3$ and $v = 7$, respectively. We further subdivide the set of vertices according to their physical interpretation. For a vertex $v \in \mathcal{V}$ we define its degree as the total number of connected pipes. We denote the degree of v by $|\cdot|$. Any vertex of degree one, i.e., $|\delta_v^+ \cup \delta_v^-| = 1$, is either an inflow ($\delta_v^- \cap \mathcal{J} = \emptyset$, vertices $v = 1$ and $v = 5$ in the example network of figure 1) or outflow boundary node ($v = 3, v = 7$). The set of such nodes is denoted by $\mathcal{V}_I$ (e.g. gas providers) and $\mathcal{V}_O$ (e.g. customers) respectively. Further, we assume that each node $v \in \mathcal{V}_C \subset \mathcal{V}$ for some set $\mathcal{V}_C$ and with degree two is a compressor station (in the example of figure 1, $\mathcal{V}_C = \{6\}$). The remaining nodes $v \in \mathcal{V}_P := \mathcal{V} \setminus (\mathcal{V}_C \cup \mathcal{V}_I \cup \mathcal{V}_O)$ are simple pipe–to–pipe intersections.

We assume the linear model (2) with equation of state (3) on each edge j of the network

$$\partial_t \rho_j + \partial_x q_j = 0 \tag{6a}$$

$$\partial_t q_j + a^2 \partial_x \rho_j = -f_g \frac{q_j |q_j|}{2D\rho_j}, \tag{6b}$$

for $x \in I_j$ and $t \in [0, T]$ and for some initial conditions

$$\rho_j(x, 0) = \rho_{j,0}(x),\ q_j(x, 0) = q_{j,0}(x). \tag{7}$$

Further, boundary conditions at $x = x_j^{a,b}$ have to be imposed. Typically, it is reasonable to prescribe the pressure $p(\rho_j) = a^2\rho_j$ for the gas providers, i.e.,

$$\rho_j(x,t) = \rho_{j,v}(t),\ x = x_j^a,\ j \in \delta_v^+,\ v \in \mathcal{V}_I \tag{8}$$

and the gas throughout q_j at the customer nodes, i.e.,

$$q_j(x,t) = q_{j,v}(t),\ x = x_j^b,\ j \in \delta_v^-,\ v \in \mathcal{V}_O. \tag{9}$$

Other choices are possible but not considered here. The boundary conditions at $x = x_j^{a/b}$ with $j \in \delta_v^\pm$ and for $v \in \mathcal{V}_P$ are obtained by prescribing (algebraic) coupling conditions at a vertex. Different conditions have been suggested and discussed in the recent literature, c.f. [5, 6, 12, 13, 14]. Here, we make the following assumptions which are commonly used in the engineering literature, see [15, 44].

(A1) $\rho_j > 0$, i.e. the solution cannot have vacuum states.
(A2) The pressure is constant at pipe-to-pipe intersections, in the sense that, at any time t the trace of the pressure functions coincide at a pipe–to–pipe intersection (see equation (10b))
(A3) Mass is conserved at pipe–to–pipe intersections (see equation (10a))

Remark 1. Condition (A1) is imposed to obtain physical solutions. However, for the linear model considered here, this condition is only relevant at compressor stations as for example seen in figure 2: If we increased the compressor with $P >> 1$ we would generate a backwards moving wave with negative density on pipe one. Recent investigations on alternatives to assumption (A2) in the case of (1) can be found in [14]. However, in the case of (6) the conditions (A2) can be obtained by the following procedure (see [33]): Since the intersection is a point of length zero we neglect the friction term at the intersection for the following considerations. Then, the momentum equation in the weak form for a single vertex v gives

$$\sum_{j\in\delta_v^\pm} \int_0^T \int_{a_j}^{b_j} \partial_t\phi_j q_j + \partial_x\phi_j\left(p(\rho_j)\right) = 0$$

for any set of test functions $\{\phi_j\}_{j\in\delta_v^\pm}, \phi_j \in C_0^\infty([a_j,b_j]\times(0,T))$. Suppose now that $a_j = b_i = 0$ for $j \in \delta_v^+$ and $i \in \delta_v^-$ and $b_j - a_j = 1$ for all $j \in \delta_v^\pm$. Then, we can choose an arbitrary function $\phi \in C_0^\infty([0,1)\times(0,T))$, arcs $k,l \in \delta_v^\pm$ and obtain for $\phi_i \equiv 0, i \neq k, i \neq l,\ \phi_k = \phi,\ \phi_l = -\phi$ the relation

$$\int_0^T \phi(0,t)\left(p(\rho_k(0,t)) - p(\rho_l(0,t))\right) = 0.$$

This gives a mathematical justification for the condition (A2).

The previous assumptions motivate the following definition of a solution $U_j = (\rho_j, q_j)$ at a single vertex $v \in \mathcal{V}_P$.

Definition 1. Consider a single vertex $v \in \mathcal{V}_P$ and assume given constant initial data U_j^0 on each edge $j \in \delta_v^- \cup \delta_v^+$ with $\rho_j^0 > 0$. A family of functions $(U_j)_{j\in\delta_v^-\cup\delta_v^+}$ is called a solution at the vertex if U_j is a weak solution in pipe j and for U_j sufficiently regular: For all $j \in \delta_v^-$, for all $i \in \delta_v^+$ and any $t > 0$ the following equations hold

$$\sum_{j\in\delta_v^-} q_j(x_j^b,\,t) = \sum_{i\in\delta_v^+} q_i(x_i^a,\,t), \tag{10a}$$

$$p(\rho_j(x_j^b,\,t)) = p(\rho_i(x_i^a,\,t)). \tag{10b}$$

In proposition 1 we show that in fact **(A2)**–**(A3)** yield boundary conditions for (6). The following propositions can also be formulated in the notion of special Riemann Solvers (RS) at the intersection [11] or as half–Riemann problems [29]. Due to the linearity of the equations and the fact that the wave speeds in the solution are $\pm a$ it suffices to give the construction of the boundary values.

Proposition 1. *Consider a vertex $v \in \mathcal{V}_P$ of degree $|v| = n$ and let U_i^0 $i = 1, \dots, n$ be constant initial data satisfying **(A1)**. Assume furthermore $f_g = 0$. Then there exists a unique solution U_j, $j = 1, \dots, n$ in the sense of Definition 1 for all $t > 0$.*

Proof. We construct solutions such that the conditions (10) are fulfilled for all $t > 0$ by prescribing boundary values at $x = x_j^a$ and $x = x_j^b$, respectively. Let $q_k^j(\rho)$ be the parameterization of the k-contact discontinuity curve ($k = 1, 2$) through the given initial state U_j^0 in the (ρ, q)-plane. Then,

$$\sum_{j \in \delta_v^-} q_1^j(\rho) = \sum_{i \in \delta_v^+} q_2^i(\rho).$$

has a unique solution $\bar{\rho}$ since the eigenvectors of ∇F are linearly independent. Here, F is given by equation (4). Finally, the boundary values for pipe j are $\bar{U}_j = \begin{pmatrix} \bar{\rho} \\ q_k^j(\bar{\rho}) \end{pmatrix}$. □

In the case $|v| = 2$ the solution obtained by applying proposition 1 is the same as to a classical Riemann problem for equation (6) with initial data U_1^0 for $x \leq 0$ and U_2^0 for $x > 0$, respectively.

Finally, it remains to discuss boundary values for edges connected to vertices $v \in \mathcal{V}_C$, i.e., the compressor stations. We introduce the (non–negative) time–dependent functions $P_v(t)$ for each $v \in \mathcal{V}_C$ modeling the applied compressor power at time t. For an applied power $P = P_v(t)$ an ideal compressor station increases an incoming pressure p_{in} to p_{out} according to [41]:

$$P = cq\left(\left(\frac{p_{out}}{p_{in}}\right)^{\kappa} - 1\right).$$

Herein, c is a compressor dependent constant and $\kappa = \frac{\gamma - 1}{\gamma}$ and γ is the isentropic coefficient, i.e., depending on the gas $\gamma \in \{5/3, 7/5\}$. We refer to [41, 25] for more details. Similar to the previous approach we obtain boundary conditions from the assumptions of mass conservation and the algebraic relation for the compressor power. The following definition allows for well–defined boundary conditions for (6) as stated in proposition 2.

Definition 2. Consider a vertex $v \in \mathcal{V}_C$ with incoming pipe $i \in \delta_v^-$ and outgoing pipe $j \in \delta_v^+$ with constant states U_i^0 and U_j^0. Let $P_v(t) > 0$ be a given function. Then, the functions U_i and U_j are called solution at the vertex $v \in \mathcal{V}_C$ if they are weak solutions on the pipe, satisfy assumption **(A1)** and fulfill

$$\begin{aligned} q_i\left(x_i^b, t\right) &= q_j\left(x_i^a, t\right) \\ cq_i\left(x_i^b, t\right)\left(\left(\frac{\rho_j\left(x_j^a, t\right)}{\rho_i\left(x_i^b, t\right)}\right)^{\kappa} - 1\right) &= P_v(t) \end{aligned} \tag{11}$$

Remark 2. In the case $P = 0$ we recover the coupling conditions (10) for junctions with two pipes.

Proposition 2. *Consider a vertex $v \in \mathcal{V}_C$ and let $U_1^0 = (\rho_1^0, q_1^0)$ and $U_2^0 = (\rho_2^0, q_2^0)$ be initial states of pipe 1 and 2 respectively, satisfying*

$$q_1^0 + q_2^0 - a\left(\rho_1^0 - \rho_2^0\right) \neq 0. \tag{12}$$

Assume furthermore $f_g = 0$. Then, for any constant $P \geq 0$ sufficiently small, there exists a unique solution U_i, $i = 1, 2$ in the sense of Definition 2 for all $t > 0$.

Before giving the formal proof we illustrate the idea of the proof in Figure 2. Therein U_1^0 and U_2^0 denote the initial states, U_m is the intersection of $U_1(\xi)$ and $U_2(\tau)$. Note that for $P = 0$ (no compressor), this state is the right boundary condition for pipe one and the left boundary condition for pipe two. Condition (12) insures $q_m \neq 0$, so that condition (11) can be fulfilled. Now, for $P = 1$ we obtain the states $\bar{U}_1$ and $\bar{U}_2$. According to the figure, we can connect U_1^0 to $\bar{U}_1$ by a 1-wave of negative speed and similarly, $\bar{U}_2$ to U_2^0 by a 2–wave of positive speed. Furthermore, $\bar{U}_1$ and $\bar{U}_2$ are such that (11) are satisfied.

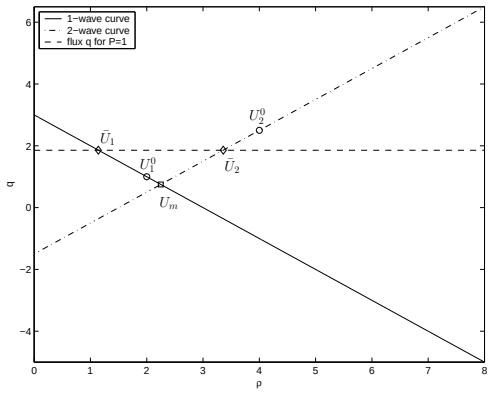

FIGURE 2. Influence of a compressor on the solution near a vertex

Proof. The case $P = 0$ is included in proposition 1 for $n = 2$. Let $P \neq 0$ and let $U_1(\xi)$ and $U_2(\tau)$ be a parameterization of the 1- and 2-wave curves through the states U_1^0 and U_2^0, given by (5). Let $U_m := (\rho_m, q_m) = U_1(\xi_m) = U_2(\tau_m)$ be the unique intersection point of curves $\xi \to U_1(\xi)$ and $\tau \to U_2(\tau)$.

The pressure condition at the vertex v as function of ξ and τ is given by

$$c\left(q_1^0 - a\xi\right)\left(\left(\frac{\rho_2^0 + \tau(\xi)}{\rho_1^0 + \xi}\right)^{\kappa} - 1\right) = P$$

or equivalently

$$\tau(\xi) = \left(\rho_1^0 + \xi\right)\left(\frac{P}{c\left(q_1^0 - a\xi\right)} + 1\right)^{\frac{1}{\kappa}} - \rho_2^0$$

for $q_1^0 - a\xi \neq 0$. If we define

$$f(P, \xi) = q_1(\xi) - q_2(\tau(\xi)) = q_1^0 - a\xi - q_2^0 - a\tau(\xi),$$

then clearly $f(0, \xi_m) = 0$ and $\frac{\partial f}{\partial \xi}(0, \xi_m) = -2a < 0$ for all U_i^0. By applying the implicit function theorem we obtain unique values (ξ, τ) for the compressor coupling and for $P \geq 0$ sufficiently small. The corresponding boundary values for (6) are therefore $U_1(\xi(P))$ and $U_2(\tau(\xi(P)))$ for pipe one and two, respectively. □

Remark 3. Typically, compressors are accompanied by bypass pipes in case of change in the flow direction. The compressor stations work only one–way. Assuming that the compressor works for $u_j > 0, t > 0$, we obtain the necessary condition $q_1^0 - a\xi_m > 0$ which in turn yields $q_1^0 + q_2^0 - a\left(\rho_1^0 - \rho_2^0\right) > 0$ as conditions on the initial states U_1^0 and U_2^0.

Finally, we comment on other approaches to treat the model equations.

Remark 4. We present a gas model based on the linear Euler equations (2, 3). In the case of the isothermal Euler equation (1) results similar to proposition 2 and 1 have been obtained in [25] and [5], respectively. Since (2) is linear, we could also introduce the characteristic variables $w^{\pm} := \rho \pm (\rho u)/a$ and analyze the system in diagonal form. Of course, we would obtain the same results. But since the physical quantities for pipe–to–pipe intersections are ρ and ρu we prefer to use (2, 3).

3. The Optimization Problem And Adjoint Equations.

In this section we propose an optimization problem for the compressor power P_v subject to the gas model introduced above. We further derive the optimality system and discuss properties of the adjoint equations.

The motivation for the optimization is as follows: The main interest of gas providers is to minimize the compressor power such that certain desired output pressures at the customer nodes are guaranteed. This problem has been studied in the context of mixed–integer optimization in [35] and in the context of fully discretized equations in [16]. Here, we use similar cost functionals and constraints as in the given references but deal with the continuous setting.

We assume each compressor $v \in \mathcal{V}_C$ to be controlled independently by prescribing a time–dependent compressor power $P_v(t)$ and define $P(t) := (P_v(t))_{v\in\mathcal{V}_C}$. We assume that each customer has a known desired pressure consumption $R_j(t)$ for $j \in \delta_v^-, v \in \mathcal{V}_O$. We further assume that the desired pressure can be delivered by suitable compressor controls. As a first step we consider a cost functional of tracking–type for the desired pressure (see below for a discussion).

$$\begin{aligned} J(P,U) \quad = \quad & \sum_{v\in\mathcal{V}_C} \int_0^T \omega_v P_v(t)\, dt \\ & + \sum_{j\in\delta_v^-, v\in\mathcal{V}_O} \int_{x_j^a}^{x_b^j} \int_0^T \frac{\alpha_j}{2} \left(p(\rho_j(x,t)) - R_j\right)^2 dxdt \\ & + \sum_{i\in\delta_v^-, v\in\mathcal{V}_O} \int_0^T \frac{\alpha_v}{2} \left(p(\rho_i(x_i^b,t)) - R_i\right)^2 dt \end{aligned}$$

where $U = (U_j)_{j\in\mathcal{J}}$, for given non–negative weights $\omega_v(t), \alpha_j(x,t)$ and $\alpha_v(t)$. The optimization problem then reads

$$\min J(P,U) \text{ subject to } (6), (7), (8), (9), (10) \text{ and } (11) \tag{14}$$

Some comments are in order.

Firstly, we use the time–dependent compressor power as control for our problem. For any fixed function $P_v(t)$ we can compute the solution to the partial differential equations (6) with the coupling conditions (10) and (11). Then, we can evaluate the cost functional. Further, we also evaluate its gradient with respect to the compressor control by means of the adjoint calculus introduced below. This information is then

used to apply steepest descent type methods for numerically solving problem (14), see section 4 and e.g. [42].
Second, we use the L_2-norm to measure the difference between applied and desired pressure on some part of the customers pipe as well as directly at the customers node. This straightforward choice allows for a convex differentiable cost functional and therefore regularizes the optimization problem. A more realistic modeling would prescribe the customers desired pressure as state constraints, i.e.,

$$p(\rho_j(x_j^b,t)) \geq R_j(t)\ j \in \delta_v^-,\ v \in \mathcal{V}_O.$$

However, due to the finite speed of propagation this constraint is clearly violated for a certain time interval, if the initial data does not fulfill this restriction, see also section 4, figure 5.
Third, as in [35, 17] we assume a simplified, linear relation between the assigned compressor power $P_v(t)$ at time t and compressor $v \in \mathcal{V}_C$ and the corresponding costs. These costs typically arise from fuel used by the compressor station. For high–pressure gas pipes so–called turbo–compressors are used [16, 17]. This type of compressor station is modeled as single idealized compressor with a constant efficiency and fuel consumption linearly related to the compressor power. Hence, the factor ω_v measure the costs per consumed fuel unit.
Fourth, there is no physical meaning of $P < 0$. Hence we additionally enforce the control constraint

$$P \geq 0$$

and present the changes to the optimality system in remark 5.

Derivation of the adjoint equations. In the sequel, we first formally derive the adjoint equations and then discuss their analytical properties. Denote by $\Phi_j = (\varphi_j, \psi_j)$ the Lagrange multiplier for density ρ_j and flux q_j, respectively. Then, the Lagrange functional is given by

$$\mathcal{L} := J(P,U) - \sum_{j\in\mathcal{J}} \int_0^T \int_{x_j^a}^{x_j^b} \begin{pmatrix} \partial_t\rho_j + \partial_x q_j \\ \partial_t q_j + \partial_x a^2\rho_j + \frac{f_g}{2D}\frac{q_j|q_j|}{\rho_j} \end{pmatrix}^T \cdot \begin{pmatrix} \varphi_j \\ \psi_j \end{pmatrix} dxdt$$

The following optimality system can be derived:

- On each pipe $j \in \mathcal{J}$ the forward equations are

$$\partial_t\rho_j + \partial_x q_j = 0,\ \partial_t q_j + a^2\partial_x\rho_j = -f_g\frac{q_j|q_j|}{2D\rho_j}$$

with initial conditions $\rho_j(x,0) = \rho_{j,},\ q_j(x,0) = q_{j,0}$ and the adjoint equations are

$$-\partial_t\psi_j - \partial_x\varphi_j = -f_g\frac{|q_j|}{D\rho_j}\psi_j, \tag{15a}$$

$$-\partial_t\varphi_j - a^2\partial_x\psi_j = f_g\frac{q_j|q_j|}{2D\rho_j^2}\psi_j + \delta_{i,j}\ \alpha_i\ a^2\ (p(\rho_i(x,t)) - R_i) \tag{15b}$$

Therein, $i := j$ if and only if $j \in \delta_v^-$ for some $v \in \mathcal{V}_O$. The terminal conditions are $\varphi_j(x,T) = 0,\ \psi_j(x,T) = 0$.
- For any vertex in $v \in \mathcal{V}_P$, $i \in \delta_v^+$, $j \in \delta_v^-$, the following conditions hold for the forward

$$\sum_{i\in\delta_v^+} q_i(x_i^a,t) = \sum_{j\in\delta_v^-} q_j\left(x_j^b,t\right),\ \rho_i(x_i^a,t) = \rho_j\left(x_j^b,t\right)$$

and the adjoint problem, respectively,

$$\sum_{i\in\delta_v^+}\psi_i\left(x_i^a,t\right)=\sum_{j\in\delta_v^-}\psi_j\left(x_j^b,t\right),\ \varphi_i\left(x_i^a,t\right)=\varphi_j\left(x_j^b,t\right). \tag{16}$$

- For any vertex which is either an inflow or outflow node, we obtain conditions for the forward system

  $$\rho_j(x_j^a,t)=\rho_{j,v}(t),\ j\in\delta_v^+, v\in\mathcal{V}_I,\ q_j(x_j^b,t)=q_{j,v}(t),\ j\in\delta_v^-, v\in\mathcal{V}_O$$

  and for the adjoint system

  $$\begin{array}{ll}\varphi_j(x_j^a,t)=0, & j\in\delta_v^+, v\in\mathcal{V}_I,\\ \psi_j(x_j^b,t)=\alpha_v\left(a^2\rho_j(x_j^b,t)-R_j\right), & j\in\delta_v^-, v\in\mathcal{V}_O\end{array} \tag{17}$$

- For the controllable vertices $v\in\mathcal{V}_C$ and with $i\in\delta_v^+$, $j\in\delta_v^-$ we obtain the forward conditions as

  $$q_i\left(x_i^a,t\right) \;=\; q_j\left(x_j^b,t\right),\ P_v=c\,q_j\left(x_j^b,t\right)\left(\left(\frac{\rho_i\left(x_i^a,t\right)}{\rho_j\left(x_j^b,t\right)}\right)^{\kappa}-1\right)$$

  and the adjoint conditions as

$$\varphi_i\left(x_i^a,t\right) \;=\; \varphi_j\left(x_j^b,t\right)+\frac{a^2\psi_i(x_i^a,t)P_v(t)\rho_j(x_j^b,t)}{c\kappa q_i^2(x_i^a,t)}\left(\frac{P_v(t)}{cq_i(x_i^a,t)}+1\right)^{\frac{1}{\kappa}-1} \tag{18a}$$

$$P_v \;=\; cq_i\left(x_i^a,t\right)\left(\left(\frac{\psi_j\left(x_j^b,t\right)}{\psi_i\left(x_i^a,t\right)}\right)^{\kappa}-1\right) \tag{18b}$$

- The optimality condition reads

  $$\omega_v+\frac{a^2}{\kappa c}\frac{\rho_j\left(x_j^b,t\right)}{q_i\left(x_i^a,t\right)}\left(\frac{P_v\left(t\right)}{cq_i\left(x_i^a,t\right)}+1\right)^{\frac{1-\kappa}{\kappa}}\psi_i\left(x_a^i,t\right)=0 \tag{19}$$

  for all $v\in\mathcal{V}_C$, $i\in\delta_v^+$, $j\in\delta_v^-$.

Remark 5. If we additionally restrict P to non-negative values the optimality condition (19) changes as follows.

$$\sum_{v\in\mathcal{V}_C}\int_0^T\left(\omega_v+\frac{a^2}{\kappa c}\frac{\rho_j\left(x_j^b,t\right)}{q_j\left(x_j^b,t\right)}\left(\frac{P_v^*\left(t\right)}{cq_j\left(x_j^b,t\right)}+1\right)^{\frac{1-\kappa}{\kappa}}\psi_i\left(x_i^a,t\right)\right)\cdot\left(P_v^*-P_v\right)\,dt\geq 0 \tag{20}$$

for all $P_v\geq 0$ where $i\in\delta_v^+$ and $j\in\delta_v^-$.

There is the a further meaning of equation (19): The left–hand side of the equation is the gradient of the reduced cost functional $\tilde{J}$ with respect to $P_v(t)$. Similarly, equation (20) yields that in the case of the constraint $P_v\geq 0$ the gradient of the reduced cost functional is non–negative and vanishes for $P_v>0$.

Next, we discuss the adjoint coupling conditions and prove that these conditions yield a well–defined boundary value problem for (15). The eigenvalues of the adjoint equations are given by $\mu_{1/2}=\pm a$ and the corresponding eigenvectors are $s_{1/2}=\begin{pmatrix}\pm a\\ 1\end{pmatrix}$. This yields a parameterization of the i-contact discontinuity curve of the adjoint equations through a given state $\bar{\Phi}=\left(\bar{\varphi},\bar{\psi}\right)$ by

$$\Phi_i\left(\xi\right)=\bar{\Phi}+\xi s_i=\bar{\Phi}+\xi\begin{pmatrix}\pm a\\ 1\end{pmatrix}\quad -\infty<\xi<\infty \tag{21}$$

Analogously to the definitions 2 and 1 we define:

Definition 3. Consider a single vertex $v \in \mathcal{V}$ and assume given constant initial data Φ_j^0 on each edge $j \in \delta_v^- \cup \delta_v^+$. A family of functions $(\Phi_j)_{j\in\delta_v^-\cup\delta_v^+}$ is called a solution at the vertex $v \in \mathcal{V} \setminus (\mathcal{V}_I \cup \mathcal{V}_O)$ if Φ_j is a weak solution in pipe j and satisfies the coupling conditions (16) for $v \in \mathcal{V}_P$ or (18) for $v \in \mathcal{V}_C$ respectively (for Φ_j sufficiently regular).

The coupling conditions (16) conserve the adjoint mass and prescribe equality of the adjoint pressure. Hence, analogously to proposition 1 we obtain the well–posedness of the boundary conditions for the adjoint equations (15) on edges j connected to a vertex $v \in \mathcal{V}_P$ in the following sense:

Proposition 3. *Consider a vertex $v \in \mathcal{V}_P$ and let Φ_i^0 $i = 1, \dots, n$ be initial states and assume $f_g = 0$. Then there exists a unique solution Φ_j, $j = 1, \dots, n$ in the sense of Definition 3 for all $t \geq 0$.*

Similarly, we obtain well–defined boundary conditions for edges connected to $v \in \mathcal{V}_I \cup \mathcal{V}_O$. It remains to discuss the adjoint coupling conditions for a compressor.

Note that for $P = 0$ the coupling conditions at a compressor vertex $v \in \mathcal{V}_C$ reduce to the linear coupling conditions for standard pipe-to-pipe intersections $v \in \mathcal{V}_P$.

Proposition 4. *Consider a vertex $v \in \mathcal{V}_C$ and assume $f_g = 0$. Let Φ_1^0, Φ_2^0, U_1^0 and U_2^0 be initial states satisfying $q_1^0 + q_2^0 + a\left(\rho_1^0 - \rho_2^0\right) \neq 0$. Then, for any constant $P \geq 0$ sufficiently small, there exists a unique subsonic solution $\Phi_i = (\varphi_i, \psi_i)$, $i = 1, 2$ in the sense of Definition 3 for all $t > 0$.*

Proof. Let $\Phi_1(\xi)$ and $\Phi_2(\tau)$ be a parameterization of the 1- and 2-wave curves through the states Φ_1^0 and Φ_2^0, given by (21). Analogously to the considerations in the proof of proposition 2, we have to assure that the coupling conditions (18) are fulfilled for all $t > 0$. This means that we seek states $\bar{\Phi}_1$ and $\bar{\Phi}_2$ such that Φ_1^0 and $\bar{\Phi}_1$ are connected by a 1-wave and Φ_2^0 and $\bar{\Phi}_2$ are connected by a 2-wave.
For $P = 0$ the solution Φ_i, $(i = 1, 2)$ has to satisfy $\varphi_1\left(x_1^b, t\right) = \varphi_2\left(x_2^a, t\right)$ and $\psi_1\left(x_1^b, t\right) = \psi_2\left(x_2^a, t\right)$. Define now by $\Phi_m := (\varphi_m, \psi_m) = \Phi_1(\xi_m) = \Phi_2(\tau_m)$ the unique intersection point of $\Phi_1(\xi)$ and $\Phi_2(\tau)$. Note that $\tau(\xi_m) = \tau_m$. Then the solution Φ_i is given by the solution of the Riemann problem

$$\partial_t \Phi_i + \begin{pmatrix} 0 & a^2 \\ 1 & 0 \end{pmatrix} \partial_x \Phi = 0 \tag{22}$$

with initial conditions

$$\Phi_1(x, 0) = \begin{cases} \Phi_1^0 & x < x_1^b \\ \bar{\Phi}_1 & x \geq x_1^b \end{cases} \tag{23}$$

$$\Phi_2(x, 0) = \begin{cases} \bar{\Phi}_2 & x \leq x_2^a \\ \Phi_2^0 & x > x_2^a \end{cases} \tag{24}$$

at the vertex v for $\bar{\Phi}_1 = \bar{\Phi}_2 = \Phi_m$.
Due to proposition 2 we know that for every $P \geq 0$ sufficiently small there exist states $U_1\left(x_b^1, t\right)) = U_1\left(x_1^b, t, P\right)$ and $U_2\left(x_2^a, t\right) = U_2\left(x_2^a, t, P\right)$ satisfying the coupling conditions (11). Recall that, directly at the vertex, $U_1\left(x_1^b, t, P\right)$ is independent of t but not of P. To simplify the notations, we write $U_1(P) = \begin{pmatrix} \rho_1(P) \\ q_1(P) \end{pmatrix}$ instead of $U_1\left(x_1^b, t, P\right)$.

Recall that $q_1\left(x_1^b,t\right)=q_2\left(x_2^a,t\right)$ and therefore the adjoint coupling conditions at a compressor node for $P\neq 0$ are

$$\begin{aligned}\varphi_2\left(x_2^a,t\right) &= \varphi_1\left(x_1^b,t\right)+\frac{a^2\psi_2(x_2^a,t)P_v(t)\rho_1(x_1^b,t)}{\kappa c q_1^2(x_1^b,t)}\left(\frac{P_v(t)}{cq_1(x_1^b,t)}+1\right)^{\frac{1}{\kappa}-1}\\ P_v &= cq_1\left(x_1^b,t\right)\left(\left(\frac{\psi_1\left(x_1^b,t\right)}{\psi_2\left(x_2^a,t\right)}\right)^{\kappa}-1\right)\end{aligned}$$

Due to the parameterization of φ and ψ, we get $\psi_1(\xi)=\psi_m+\xi$ and $\varphi_1(\xi)=\varphi_m-a\xi$ for some ξ and $\psi_2(\tau)=\psi_m+\tau$ as well as $\varphi_2(\tau)=\varphi_m+a\tau$ for some τ. We can thus express the coupling condition in terms of φ_i and ψ_i to get an expression for τ in terms of ξ.

$$\tau(P,\xi)=\left(g\left(P,q_1(P)\right)^{\frac{1}{\kappa}}-1\right)\psi_m+g\left(P,q_1(P)\right)^{\frac{1}{\kappa}}\xi,$$

where $g\left(P,q_1(P)\right)=\left(\frac{P}{cq_1(P)}+1\right)$. Define

$$f(P,\xi)=\varphi_1(\xi)+\frac{a^2P\rho_1(P)}{\kappa cq_1^2(P)}g\left(P,q_1(P)\right)^{\frac{1-\kappa}{\kappa}}\psi_2\left(\tau(P,\xi)\right)-\varphi_2\left(\tau(P,\xi)\right)$$

Then clearly $f(0,\xi_m)=0$ since $\tau(\xi_m)=\tau_m$ and

$$\frac{\partial}{\partial\xi}f(P,\xi)=-a\left(1+g\left(P,q_1(P)\right)^{\frac{1}{\kappa}}\right)-\frac{a^2P\rho_1(P)}{\kappa cq_1^2(P)}g\left(P,q_1(P)\right)^{\frac{2-\kappa}{\kappa}},$$

since $\frac{d}{d\xi}\psi\left(\tau(P,\xi)\right)=g\left(P,q_1(P)\right)^{\frac{1}{\kappa}}$.
Note that $\frac{\partial}{\partial\xi}f(0,\xi_m)=-2a$. Using the implicit function theorem we now conclude the existence of a neighborhood $\mathcal{B}(0)\subset\mathbb{R}$ and a function $\xi:\mathcal{B}(0)\to\mathbb{R}$ mapping P onto $\xi(P)$ with $\xi(0)=\xi_m$ and $f\left(P,\xi(P)\right)=0$ for all $P\in\mathcal{B}(0)$. This yields the solvability of the compressor coupling conditions (18) for P sufficiently small. The solutions Φ_1 and Φ_2 are then given by the solution to the Riemann problem (22), (23), (24) for $\bar{\Phi}_1=\begin{pmatrix}\varphi_1(\xi(P))\\ \psi_1(\xi(P))\end{pmatrix}$ and $\bar{\Phi}_2=\begin{pmatrix}\varphi_2(\tau(P,\xi(P)))\\ \psi_2(\tau(P,\xi(P)))\end{pmatrix}$. □

4. **Numerical Examples.** We present numerical examples for solutions to the optimization problem (14). We discretize the optimality system ('optimize–then–discretize') using a second–order relaxed finite volume scheme, see [7, 31, 34]. For the simplified model this reduces to a second–order upwinding scheme with minmod–limiter. The source term is integrated exactly in the case of the forward equation (6) and an explicit forward Euler discretization in case of the adjoint equation (15). The cost functional is discretized using a second–order quadrature rule. The optimization is carried out for the reduced cost functional using a steepest descent method with second–order correction, see [32, 36]. The optimization is terminated if the projected gradient is less than the tolerance *tol* in the L_2-norm. Further parameters are $\kappa=\frac{2}{7},a=1,c=1,D=\frac{1}{2}$ and $x_j^b-x_j^a=1$ for all pipes. The examples will be presented for the simple test case of two connected pipes with a single compressor station as depicted in figure 3. The cost functional is given by (13) with $\omega_\nu=1$, $\alpha_j=0$ and $\alpha_v=100$.

FIGURE 3. Sample network with a single compressor station.

Verification of adjoint equations. At first we verify the adjoint calculus by comparing with a finite difference approximation of the gradient. The cost functional is given by (13) and using the adjoint calculus its reduced gradient is given by (20). We compare both gradients using $N_x \times N_t = 11 \times 27 = 297$ discretization points and a network consisting of two arcs connected by a compressor. We report the gradient for a given compressor control with starting value $P = 0$ in figure 4 and observe a good agreement between the finite difference approximation to the gradient and the adjoint calculus. We emphasize that the computation of the gradient using the adjoint calculus only requires to solve once (6) and once (15) independent of the number N_t of discretization points for the compressor control $P_v^i = P_v(t_i)$. However, using a central finite difference approximation the gradient approximation needs $2 \cdot N_t$ computations of (6).

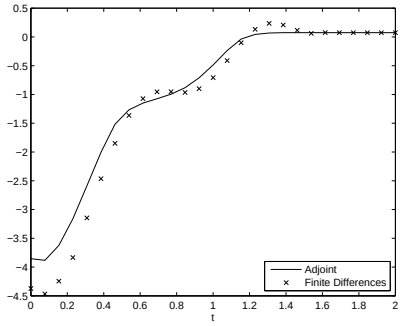

FIGURE 4. Comparison between gradient computed by the adjoint method (solid line) and a finite difference approximation of the gradient (dashed line)

Time–dependent optimization results. Initially, we assume that the compressor is turned off and the network is at steady state with an outflow pressure of $p(\rho(a_1, 0)) = 3$ and a flux of $q_2(b_2, 0) = 15$ at the customer. Then, the pressure profile along the pipe is square–root shaped and decreasing to nearly $\frac{1}{2}$ at $x = b_2$. We prescribe a time horizon of $T = 2$ and assume that customer requires a pressure distribution as depicted in the lower right part of figure 5. We solve the optimization problem for the time–dependent compressor energy $P_v(t)$ on a grid $N_x \times N_t = 100 \times 264$ per pipe. The optimization with initial guess $P_v(t) \equiv 0$ terminates within a tolerance of 10^{-2} using 92 iterations. The optimal compressor energy $P_v^*(t)$ is depicted in the lower left part of figure 5. Further, we report the corresponding optimal density and flux evolution in the top part of this figure. We observe the expected results: Since wave speeds and length of the pipe are equal, any change in the compressor energy at time $t > 1$ does not reach the boundary $x = b_2$ within the given time interval $T = 2$. Therefore, the compressor energy drops down to zero at $t \approx 1$. Similarly, in the comparison of the finally obtained pressure at $x = b_2$ and the desired pressure

we again observe that changes in the compressor energy only affect the outlet pressure for $t > 1$. The emerging of waves introduced by turning on the compressor can be observed in the contour plots for density and flux. The emerging waves reach the boundary of the computational domain and interact with the boundary conditions which can yield traveling waves and yields the zig zag pattern. At $x = 1$ the pipes one and two are coupled by the compressor. We observe the equal flux through $x = 1$ as prescribed by the coupling condition (11) as well as the discontinuity in the density as long as the compressor is turned on, i.e. for $t \leq 1$.

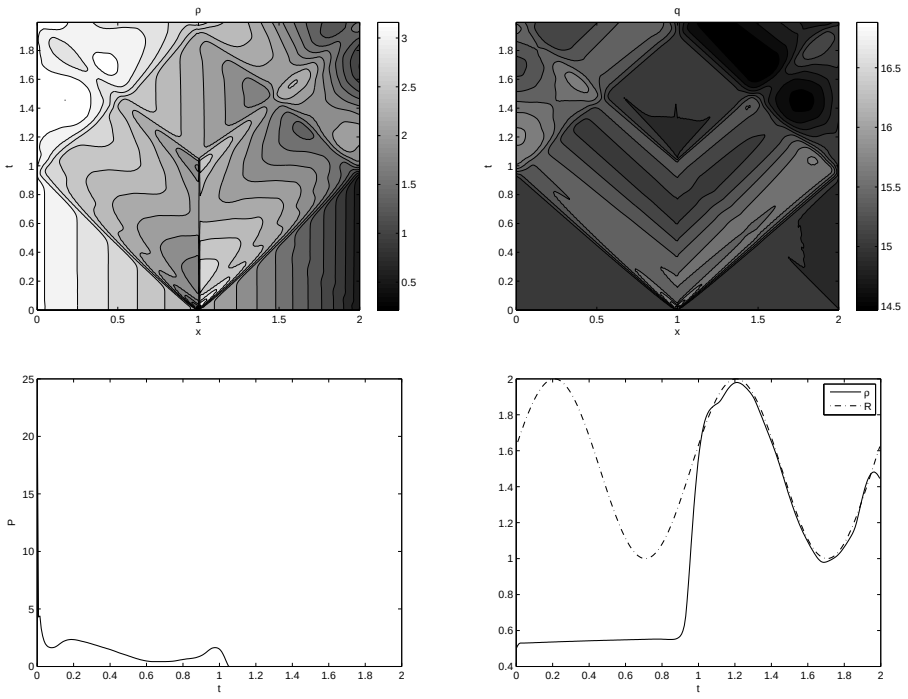

FIGURE 5. Results on transient gas flow for network (3). Arc one and two correspond to $x \in (0, 1)$ and $x \in (1, 2)$, respectively. The optimal pressure control $P_v^*(t)$ is given in the lower left plot, the corresponding density and flux evolutions in the upper left and upper right part. The desired pressure at $x = b_2$ and the actual achieved pressure are depicted in the lower right part.

Comparison to the steady–state optimization problem. Depending on the size of the network and the discretization, problem (14) can be computationally expensive to solve and the question arises whether or not one can replace the already simplified dynamics by an even simpler one. On the toy problem (figure 3) we compare the impact of the transient model with a coarser model. The coarse model is obtained assuming a steady–state inside each pipe. Then, (6) reduces to an ordinary differential equation for the pressure loss along the pipe. To be more precise, a steady–state solution $U_j = (\rho_j(x), q_j(x))$ on pipe j to equations (6) satisfies

$$q_j = \text{ const } , \ \partial_x p(\rho_j) = -\frac{f_g q_j |q_j|}{2D\rho_j}, \tag{25}$$

where the flux q_j is determined by the boundary condition. Again, we couple this model using the conditions (10) and (11). In our example given by figure 3, the pressure on the customer's pipe ($j = 2$) can be computed exactly by solving (25), (11), (9), (8). The pressure on the customer pipe is then given by

$$\begin{aligned} p^2(\rho_2(x)) &= -\frac{f_g a^2 q_{2,0}|q_{2,0}|}{D}(x - x_2^a) \\ &\quad + \left(p^2(\rho_{1,0}) - \frac{f_g a^2 q_{2,0}|q_{2,0}|}{D}(x_1^b - x_1^a)\right)\left(\frac{P_v}{cq_{2,0}} + 1\right)^{\frac{2}{\kappa}}, \end{aligned}$$

for $x \in [x_2^a, x_2^b]$, possibly time–dependent inlet pressure of $p(\rho_{1,0})$, outlet flux of $q_{2,0}$ and compressor energy P_v. Using the same cost functional as in (14), the optimization problem reads

$$\min J(P, U) \text{ subject to } (25), (7), (8), (9), (10) \text{ and } (11) \tag{26}$$

In the following, we compare the solutions to (14) and (26). In the latter case the solution is obtained by a quasi–Newton descent method, see [32] up to order 10^{-6}. We use the same boundary data as before and consider an optimization horizon of $T = 3$. The desired state R_i is given by $R_i = \frac{3}{2} + \frac{1}{2}\sin\left(2\pi t + \frac{1}{4}\right)$ as in the previous example. The solution on $[0, 2]$ to (26) is depicted in figure 6. In contrast to the transient case there is no delay due to traveling waves and the compressor power is such that the desired pressure is instantaneously obtained. Hence, the optimal compressor power has also a sinusoidal shape. Next we compare the optimal compressor power obtained when solving (14) with (26) in figure 7. We observe some differences. Qualitatively they are similar, but due to the induced dynamics in the transient model there are quantitative differences. The effect of the quantitative differences is observed in the right part of figure 7. Therein, the optimal control obtained for the *steady–state* model, i.e. (26), is used as compressor control for the *dynamic* model, i.e., (6). Comparing this with the right part of figure 5 we observe a rather huge difference between the actual pressure at the customer and the desired pressure. This indicates that there are significant differences between solutions to problems (14) and (26) even so their qualitative behavior is similar. In this example the coarse model (25) cannot provide reasonable optimal controls for the full transient model (6).

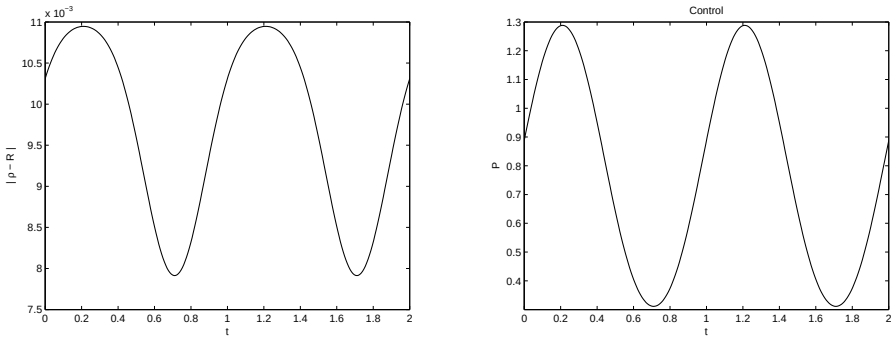

FIGURE 6. Results on problem (26). Difference between desired and actual pressure profile at the customer (to the left) and corresponding optimal compressor power $P_v^*(t)$ (to the right).

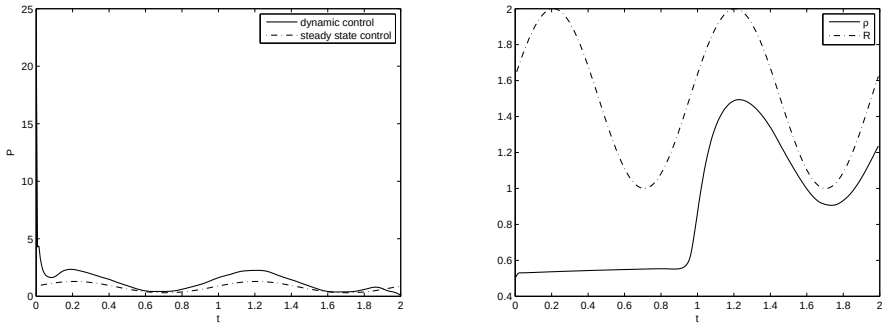

FIGURE 7. Comparison of the optimal compressor power of (26) (dashed line) and (14) (solid line) in the left part. Outflow pressure using model (6) with the optimal compressor power obtained from (26).

Comparison of nonlinear, simplified and steady–state models. As stated in the introduction, the model under consideration is a simplification of the isothermal Euler equations. In this section we compare the qualitative and quantitative difference between the full nonlinear model (1), the simplified model (2) discussed in this work and the steady–state problem (25). We compare the models under realistic conditions taken from [9, 39]: Each pipe has a length $x = 100[m]$, the speed of sound is $a = 300[m/s]$. The inlet pressure is $p(\rho(x_1^a, t)) = 40[bar]$ and the outlet flux is $q(x_2^b, t) = 3.74\ 10^5[m^3/h]$ under standard conditions. The friction factor is $f_g = 1.1\ 10^{-2}$.

In order to investigate the dependence on the optimal compressor power we consider a situation as in figure 3. Therein, a single compressor connects two pipes. We prescribe the inlet pressure and the outlet flow with values stated above. We assume an optimal compressor power control as

$$P_v(t) = \frac{1}{2} + \frac{1}{4}\sin(\pi\frac{t}{2})$$

and a time horizon of $T = 4[min]$. We simulate the nonlinear model (1), the simplified model (2) and the steady–state model (25) with the given control. We refer to [25] for a discussion of the necessary compressor coupling conditions for the isothermal Euler equations. We present results on the outlet pressure for all simulations in figure 8. For a detailed comparison of the pressure evolution for the isothermal and simplified model in each pipe we refer to figure 9. Under the given flow conditions we observe a qualitative and quantitatively good agreement between the isothermal and the simplified model. Peaks and sinks in the final pressure evolution are captured by the simplified model. The maximal difference in pressure at the outlet is less than $2[bar]$ corresponding to an error of less than 5%. This is even true for the full time evolution of the problem as seen in figure 9. This supports the fact that in realistic flow regimes the nonlinear momentum can be neglected without losing qualitative features of the solution. As already seen in the previous example and as expected the steady–state approximation is rather inaccurate and cannot capture the detailed dynamics.

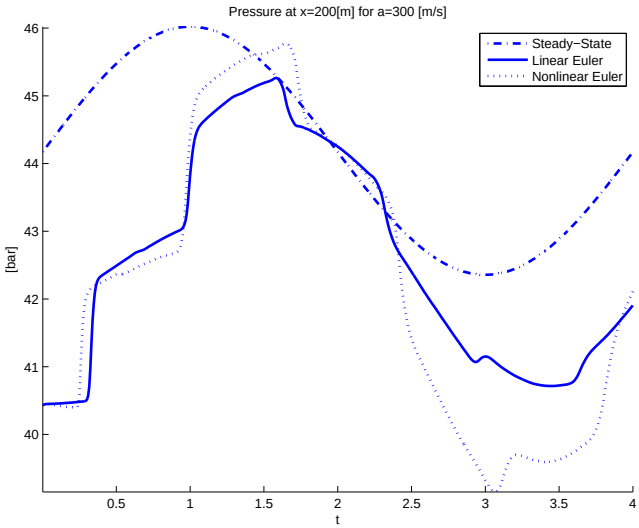

FIGURE 8. Comparison of outlet pressures $p(\rho(x_2^b, t))[bar]$ for simulations of isothermal, simplified and steady–state model. In all cases the same compressor power is applied.

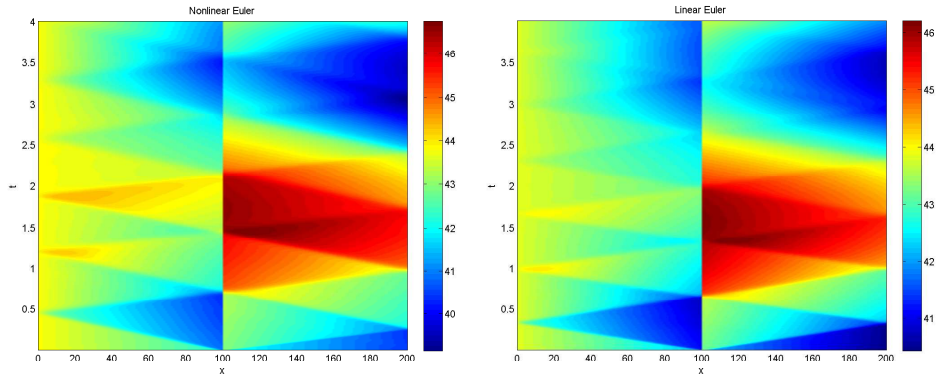

FIGURE 9. Simulation results for the pressure in the isothermal and simplified model, respectively. The same compressor power and the same boundary conditions are applied in both cases. The location of the compressor is at $x = 100$.

5. **Summary.** We presented an optimization problem for a simplified model used in gas dynamics on networks with compressor stations. We derived an adjoint calculus and provided an analysis using the coupling conditions arising. The derived equations have been implemented and tested on a small toy example to illustrate the qualitative behavior of the expected solutions. A comparison with a steady–state optimization is provided.

Acknowledgments. This work has been supported by the DFG priority program SPP 1253, 'Optimization of partial differential equations'.

REFERENCES

[1] C. D'Apice and R. Manzo, *A fluid dynamic model for supply chains*, Networks and Heterogenous Media, **1** (2006), 379–398.

[2] C. D'Apice and R. Manzo, *Calculation of predicted average packet delay and its application for flow control in data network*, J. Inf. Optimization Sci., **27** (2006), 411–423.

[3] D. Armbruster, P. Degond and C. Ringhofer, *A model for the dynamics of large queuing networks and supply chains*, SIAM J. Appl. Math., **66** (2006), 896–920.

[4] D. Armbruster, P. Degond and C. Ringhofer, *Kinetic and fluid models for supply chains supporting policy attributes*, preprint, 2005.

[5] M. K. Banda, M. Herty and A. Klar, *Coupling conditions for gas networks governed by the isothermal Euler equations*, Networks and Heterogenous Media, **1** (2006), 295-314.

[6] M. K. Banda, M. Herty and A. Klar, *Gas flow in pipeline networks*, Networks and Heterogenous Media, **1** (2006), 41–56.

[7] M. K. Banda and M. Seaid, *Higher-Order relaxation schemes for hyperbolic systems of conservation laws*, J. Numer. Math., **13** (2005), 171–196.

[8] G. Bretti, R. Natalini and B. Piccoli, *Numerical approximations of a traffic flow model on networks.*, Netw. Heterog. Media, **1** (2006), 57–84.

[9] I. Cameron, *Using an Excel-based model for Steady-State and transient simulation* Technical Report avaible at TransCanada Transmission Company, 2000.

[10] N. H. Chen, *An explicit equation for friction factor in pipe*, Ind. Eng. Chem. Fund., **18** (1979), 296–297.

[11] G. M. Coclite, M. Garavello and B. Piccoli, *Traffic flow on road networks*, SIAM J. Math. Anal., **36** (2005), 1862–1886.

[12] R. M. Colombo and M. Garavello, *A well–posed Riemann problem for the p-system at a junction*, Networks and Heterogenous Media, **1** (2006), 495–511.

[13] R. M. Colombo and M. Garavello, *On the Cauchy problem for the p-system at a junction*, preprint, 2006.

[14] R. M. Colombo and M. Garavello, *On the p-system at a junction*, Contemporary Mathematics, **426** (2007), 193–217.

[15] Crane Valve Group, *Flow of fluids through valves, fittings and pipes*, Crane Technical Paper No. 410, 1998.

[16] K. Ehrhardt and M. C. Steinbach, *KKT systems in operative planning for gas distribution networks*, ZIB Report, **04-21** 2004.

[17] K. Ehrhardt and M. C. Steinbach, *Nonlinear optimization in gas networks*, in "Modeling, Simulation and Optimization of Complex Processes" H. G. Bock, E. Kostina, H. X. Phu, R. Ranacher (ed.), 2005

[18] M. Garavello and B. Piccoli, *Source-Destination flow on a road network*, Comm. Math. Sci., **3** (2005), 261–283.

[19] M. Garavello and B. Piccoli, "Traffic Flow on Network," Applied Math Series n. 1, American Institute of Mathematical Sciences, 2006.

[20] S. Göttlich, M. Herty and A. Klar, *Network models for supply chains*, Communication in Mathematical Sciences, **3** (2006), 545–559.

[21] V. N. Gopal, *Techniques to optimize fuel and compressor combination elements*, in "American Gas Association Transmission Conference", 1979.

[22] M. Gugat, *Optimal nodal control of networked hyperbolic systems: evaluation of derivatives.*, Adv. Model. Optim., **7** (2005), 9–37.

[23] M. Gugat and G.Leugering, *Global boundary controllability of the St. Venant equations between steady states*, Annales des l'Institut Henri Poincaré, Nonlinear Analysis, **20** (2003), 1–11.

[24] M. Gugat, G. Leugering, K. Schittkowski and E. J. P. G. Schmidt, *Modelling, stabilization and control of flow in networks of open channels*, in "Online Optimization of Large Scale Systems", Grötschel, Krumke, Rambau (ed.), Springer, 2001.

[25] M. Herty, *Modeling, simulation and optimization of gas networks with compressors*, Networks and Heterogenous Media, **2** (2007), 81–97.

[26] M. Herty, M. Gugat, A. Klar and G. Leugering, *Optimal control for traffic flow networks*, Journal of Optimization Theory and Applications, **126** (2005), 589–616.

[27] M. Herty and A. Klar, *Modeling and optimization of traffic networks*, SIAM J. Sci. Comp., **25** (2004), 1066–1087.

[28] M. Herty, S. Moutari and M. Rascle, *Optimization criteria for modelling intersections of vehicular traffic flow*, Networks and Heterogenous Media, **1** (2006), 275–294.
[29] M. Herty and M. Rascle, *Coupling conditions for a class of second–order models for traffic flow*, SIAM J. Math. Anal., **38** (2007), 595–616.
[30] H. Holden and N. H. Risebro, *Riemann problems with a kink*, preprint, 1996.
[31] S. Jin and Z. Xin, *The relaxation schemes for systems of conservation laws in arbitrary space dimensions*, Comm. Pure Appl. Math., **48** (1995), 235–276.
[32] C. T. Kelley, "Iterative Methods for Optimization," SIAM Frontiers in Applied Mathematics, 1999.
[33] G. Leugering and E. J. P. G. Schmidt, *On the modelling and stabilization of flows in networks of open canals*, SIAM J. Control Optim., **41** (2002), 164–180.
[34] H. L. Liu and G. Warnecke, *Convergence rates for relaxation schemes approximating conservation laws*, SIAM J. Numer. Anal., **37** (2000), 1316–1337.
[35] A. Martin, M. Möller and S. Moritz, *Mixed Integer Models for the stationary case of gas network optimization*, Math. Programming, **105** (2006), 563–582.
[36] J. J. Moré and D. J. Thuente, *Line search algorithms with guaranteed sufficient decrease*, ACM Trans. Math. Softw., **20** (1994), 286–307.
[37] A. J. Osiadacz, *Different transient models - limitations, advantages and disadvantages*, PSIG Technical Report, (1996).
[38] A. J. Osiadacz, "Simulation and Analysis of Gas Networks," Gulf Publishing Company, Houston, 1987
[39] A. Osiadacz and M. Chaczykowski, *Comparison of isothermal and non–isothermal transient models*, Technical Report available at Warsaw University of Technology, (1998).
[40] Pipeline Simulation Interest Group, www.psig.org.
[41] M. Steinbach, *On PDE solution in transient optimization of gas networks*, Technical Report ZR-04-46, ZIB Berlin, (2004).
[42] F. Tröltzsch, "Optimale Steuerung Partieller Differentialgleichungen. Theorie, Verfahren und Anwendungen," Vieweg, Wiesbaden, 2005.
[43] Z. Vostrý, *Transient optimization of gas transport and distribution*, in "Proceedings of the 2nd International Workshop SIMONE on Innovative Approaches to Modelling and Optimal Control of Large Scale Pipeline Networks", (1993).
[44] F. M. White, "Fluid Mechanics," McGraw–Hill, New York, 2002.
[45] H. I. Zimmer, *Calculating optimum pipeline operations*, in "American Gas Association Transmission Conference", (1975).

Received March 2007; revised August 2007.

E-mail address: herty@mathematik.uni-kl.de
E-mail address: sachers@mathematik.uni-kl.de